

Synthetic Hilbert Space Engineering of Molecular Qudits: Isotopologue Chemistry

Wolfgang Wernsdorfer* and Mario Ruben*

One of the most ambitious technological goals is the development of devices working under the laws of quantum mechanics. Among others, an important challenge to be resolved on the way to such breakthrough technology concerns the scalability of the available Hilbert space. Recently, proof-of-principle experiments were reported, in which the implementation of quantum algorithms (the Grover's search algorithm, iSWAP-gate, etc.) in a single-molecule nuclear spin qudit (with $d = 4$) known as $^{159}\text{TbPc}_2$ was described, where the nuclear spins of lanthanides are used as a quantum register to execute simple quantum algorithms. In this progress report, the goal of linear and exponential up-scalability of the available Hilbert space expressed by the qudit-dimension " d " is addressed by synthesizing lanthanide metal complexes as quantum computing hardware. The synthesis of multinuclear large-Hilbert-space complexes has to be carried out under strict control of the nuclear spin degree of freedom leading to isotopologues, whereby electronic coupling between several nuclear spin units will exponentially extend the Hilbert space available for quantum information processing. Thus, improved multilevel spin qudits can be achieved that exhibit an exponentially scalable Hilbert space to enable high-performance quantum computing and information storage.

quantum mechanical principles this approach allows a subject to know the exact description of a system. This phenomenon led the renowned physicist Feynman,^[3] among others,^[4] to propose the exploitation of entanglement and/or superposition of states to perform certain computational tasks not achievable with classical computers. However, the challenge of such a proposal is the development of both hardware and software components, i.e., building blocks and algorithms, compatible to perform processing of information at the quantum level (Figure 1).

On the software side of quantum algorithms, the early developments of the quantum information processing (QIP) field were slow until 1994 when Peter Shor reported a remarkable quantum polynomial algorithm to factorize integers.^[5] This was quickly followed by Grover's quantum algorithm,^[6] which proposes the use of quantum mechanics to achieve quadratic speedup in search queries of unsorted

databases or general optimization tasks. Lloyd subsequently validated Feynman's proposition in which a quantum computer (QC) could simulate intractable quantum systems.^[7] These advantages undoubtedly led to a single conclusion: a QC and QIP can outperform classical processing schemes, computers, or algorithms in certain tasks that even extremely powerful computer clusters would not be able to perform. In March of 2018, Intel presented a 49-qubit QC chip,^[8] while IBM and other competitors were allowing to execute quantum algorithms using qubit numbers up to 19.^[9] However, it is estimated that a very large number of qubits will be needed to achieve quantum supremacy, in particular because of highly demanding error correction lines.

On the hardware side, the very special requirements of the quantum mechanical laws will necessarily lead to the development of new classes of materials as building blocks. In this context, during the last decade, several materials have been proposed as quantum bits (qubits) ranging from defects in solids,^[10–12] quantum dots,^[13,14] photons,^[15,16] impurities in solids,^[17–19] superconducting systems,^[20] trapped ions,^[21] and molecules,^[22] among others. Obviously, there is considerable motivation to produce quantum computers. This has attracted a great deal of interest from scientists working in materials science, chemistry, physics, and nanofabrication technologies. For example, the company D-wave has disclosed a quantum annealer that performs certain calculations with sufficient speed. A consortium involving Google and NASA has therefore invested large sums in such technology exhibiting still inconclusive results in terms of showing quantum advantage.^[23]


1. Introduction

The emergence of the nonindependent description of quantum states (i.e., entanglement and superposition) dates back to the time of Einstein et al.^[1] and Schrödinger.^[2] Using underlying

Prof. W. Wernsdorfer
Institute of Physics (PHI)
Karlsruhe Institute of Technology (KIT)
Wolfgang-Gaede-Str. 1, D-76131 Karlsruhe, Germany
E-mail: wolfgang.wernsdorfer@kit.edu

Prof. W. Wernsdorfer, Prof. M. Ruben
Institute of Nanotechnology (INT) and Institute of Quantum Materials and Technology (IQMT)
Karlsruhe Institute of Technology (KIT)
Hermann-von-Helmholtz-Platz 1
D-76344 Eggenstein-Leopoldshafen, Germany
E-mail: mario.ruben@kit.edu

Prof. M. Ruben
Institut de Physique et Chimie des Matériaux de Strasbourg (IPCMS)
CNRS
Université de Strasbourg
23 rue du Loess, BP 43, F-67034 Strasbourg Cedex 2, France

 The ORCID identification number(s) for the author(s) of this article can be found under <https://doi.org/10.1002/adma.201806687>.

© 2019 The Authors. Published by WILEY-VCH Verlag GmbH & Co. KGaA, Weinheim. This is an open access article under the terms of the Creative Commons Attribution-NonCommercial License, which permits use, distribution and reproduction in any medium, provided the original work is properly cited and is not used for commercial purposes.

DOI: 10.1002/adma.201806687

However, one common challenge of these different approaches toward the realization of such a break-through technology is the attempt to establish scalability of the available states, the so-called Hilbert space. This means that even when proof-of-principle studies show that quantum operations are possible, it is not clear whether the quantum principle of superposition and entanglement can be maintained in a sufficiently robust manner for larger qubit ensembles.^[24]

In this progress report, we would like to address the goal of linear and exponential up-scalability of the available Hilbert space expressed through the qudit-dimension “*d*” by synthesizing lanthanide metal complexes as quantum computing hardware. The synthesis of multinuclear large-Hilbert-space complexes has to be carried out under strict control of the nuclear spin degree of freedom leading to isotopologues, defined here as molecular entities that differ only in their isotopic composition of the central atom, whereby electronic coupling between several nuclear spin units will exponentially extend the Hilbert space available for quantum information

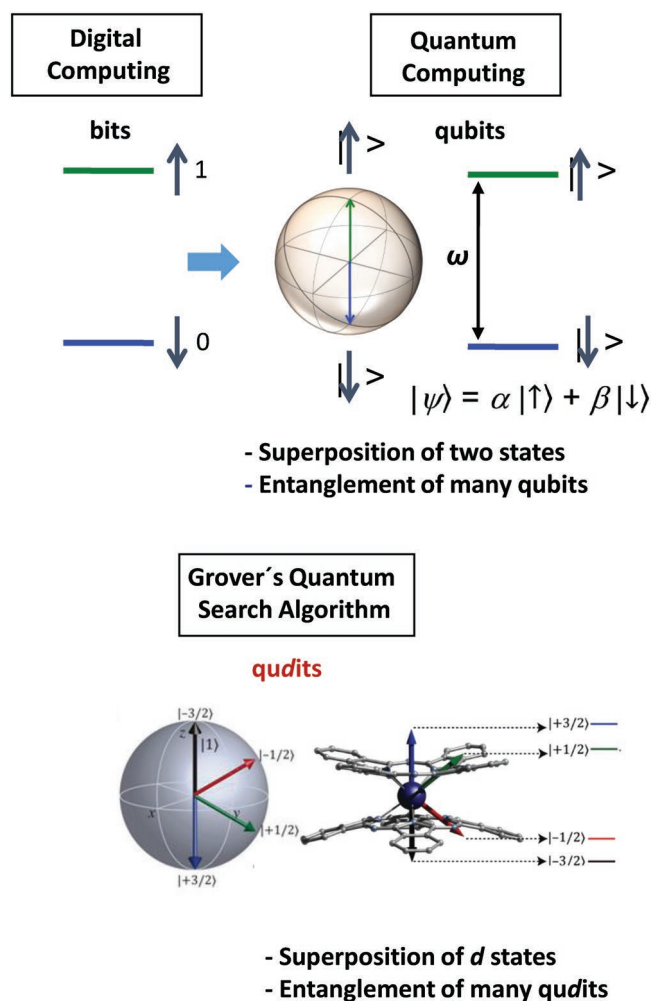


Figure 1. Top: The quantum information paradigm changing computation by going from the bit to the qubit scheme via the superposition and entanglements as quantum mechanical principles; ω representing a radio-frequency oscillating field; and bottom: from a two-level qubit scheme to a multilevel qudit (here $d = 4$).



Wolfgang Wernsdorfer, born in Germany in 1966, studied physics at the University of Würzburg and École Normale Supérieure in Lyon. In 1993, he became a doctoral researcher at the Low Temperature Laboratory and the Laboratoire de Magnetism in Grenoble, France. In 2004, he became directeur de recherche at the Institut NEEL. In 2016, he accepted a position as Humboldt Professor at the Institute of Physics and the Institute of Nanotechnology at the KIT.



Mario Ruben obtained his Ph.D. in 1998 from the University of Jena, Germany. During a DAAD post-doctoral fellowship, he worked in Prof. J.-M. Lehn's research group at the ISIS in Strasbourg, France. In 2001, he moved to the Institute of Nanotechnology in Karlsruhe and in 2010, he accepted a position as Professor at the Université de Strasbourg, France. In 2013, he became Full Professor for Molecular Materials at the Institutes of Inorganic Chemistry and of Nanotechnology at the KIT. His research interests involve the design, synthesis, and physical characterization of functional molecules and their implementation and integration into operational nanosystems.

processing. Thus, improved multilevel spin qudits can be achieved that exhibit an exponentially scalable Hilbert space that might enable high-performance quantum computing and information storage.

2. Molecular Quantum Devices

Molecular quantum magnets are considered promising quantum objects because of i) their intrinsic monodispersity and ii) the unique possibility of individualized control of the surrounding atoms. These molecular objects can be produced by synthetic techniques in a large number of identical (i.e., atomically precise) copies - a prerequisite for the scalable exploitation of the quantum properties. Devices based on single or small numbers of molecules could speed up information handling or allow new unprecedented processing schemes.

In a series of recent publications,^[25] it was shown that magnetic molecules, in particular lanthanide complexes as $^{159}\text{TbPC}_2$ single molecule magnets (SMMs), can act as active units in different molecular quantum spintronic devices as i) the molecular spin valve,^[26] ii) the molecular spin transistor,^[27,28] and iii) the molecular spin resonator.^[29] These devices show

general features of all-electrical control of a single nuclear spin qubit in a molecule. Moreover, molecule-based nuclear spins are extremely well-isolated from environmental perturbations, making them less prone to decoherence. Because these results are of general character and thus potentially transferable to other magnetic molecules, these investigations reveal new possibilities for device physics (Figure 2).

3. Molecular Systems

In our own work, we could show that the $^{159}\text{TbPc}_2$ -SMM complex fulfills all criteria to act as qudit.^[30] The $^{159}\text{TbPc}_2$ molecule is built up from an atomic core of a metal ion surrounded by a shell of organic material (Figure 3). At low temperatures, the lanthanide-based spin behaves as simple, few-level system sufficiently decoupled from the environment allowing for long decoherence times, thereby making them ideal candidates for the implementation of qudits. The $^{159}\text{TbPc}_2$ complex behaves as an SMM composed of three magnetic components: i) an $S = 1/2$ organic π -radical, which is delocalized over the two aromatic phthalocyanine (Pc) ligands. The interaction of the π -radical with the 4f-electrons of the $^{159}\text{Tb}^{3+}$ ions is antiferromagnetic in nature. ii) At the metal side, the electronic spin $J = 6$ arises from strong spin-orbit coupling with a total spin of $S = 3$ and the orbital momentum $L = 3$. The ligand field, which is generated by the two Pc ligands, leads to a well-isolated electron spin ground state doublet of $|J = +6\rangle$ and $|J = -6\rangle$ with a uniaxial anisotropy axis perpendicular to the Pc plane. iii) The twofold degeneracy of the doublet is lifted by the hyperfine coupling to the nuclear spin embodied in the lanthanide ($I = 3/2$) and splits each electronic spin ground state into four different quantum states. A nuclear spin qubit emerges from the atomic core of the $^{159}\text{Tb}^{3+}$ ion. The molecule possesses a nuclear spin $I = 3/2$ expressed as four different electromagnetic qudit states $| -3/2\rangle$, $| -1/2\rangle$, $| +1/2\rangle$, and $| +3/2\rangle$ exhibiting four avoided level crossings with a tunnel splitting of each of around 1 mK (Figure 3).

The electronic transport through single TbPc_2 molecules was realized under variable magnetic fields, thus revealing hysteretic behavior that is reminiscent of the magnetic hysteresis because of resonant quantum tunneling between hyperfine split energy levels. The experimental read-out procedure relies on the highly efficient detection of the quantum tunneling of magnetization (QTM) of the electronic magnetic moment at particular values of the magnetic field corresponding to the four avoided energy-level crossings. This is in perfect quantitative agreement with theoretical predictions. Remarkably, by recording the conductance as a function of an external magnetic field, it was possible to determine the dynamics of the four different nuclear spin states and thus to measure individual relaxation times (T_1) exceeding several tens of seconds. The experiment is found to be in good agreement with quantum Monte Carlo simulations, suggesting that the relaxation times are limited by the current traversing the transistor. As a result, the electrical read-out of time-trajectories obtained from the isolated nuclear spin $I = 3/2$ was reported. The device detects the four different nuclear spin states of the Tb(III) ion with high fidelities of 95%.^[27] Ramsey experiments allow the extraction of

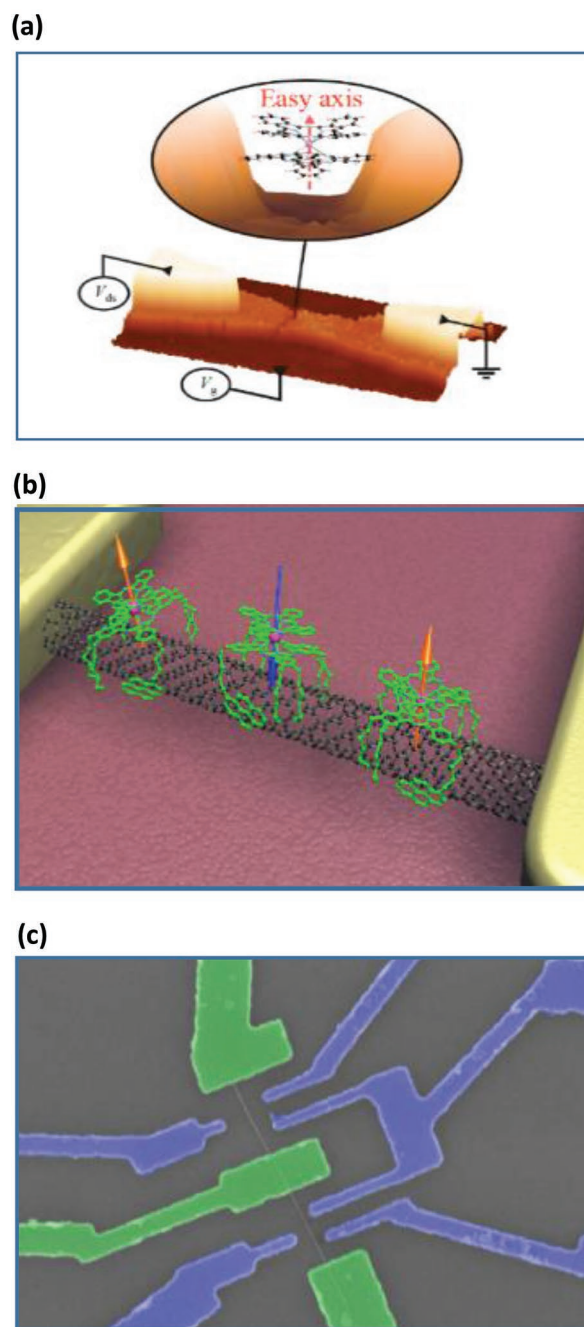


Figure 2. a) Representation of the molecular spin-transistor, in which electron transport can be controlled by an electrostatic coupling to a gate voltage. A schematic zoom into the nanogap is depicted on the upper part showing the molecular structure of the $^{159}\text{TbPc}_2$ -SMM (Pc = phthalocyanine) as well as its anisotropy axis. b) A spin-valve built entirely from molecular components: A lead made of a single-wall carbon nanotube (black in the Figure) is contacted at each end by nonmagnetic electrodes (gold color). The device is coupled laterally to $^{159}\text{TbPc}_2$ quantum magnets (green). Sweeping a magnetic field modulates the conductance through the CNT, achieving magnetoresistance ratios up to 300% between fully polarized and nonpolarized molecular configurations. c) First realization of a multigate device. The carbon nanotube is connected to three electrodes (green). Several local gates (blue) allow the tuning of the coupling between the nanotube and the $^{159}\text{TbPc}_2$ -SMMs deposited onto the nanotube.^[26–29] Panel a reproduced with permission.^[28] Copyright 2014, AAAS.

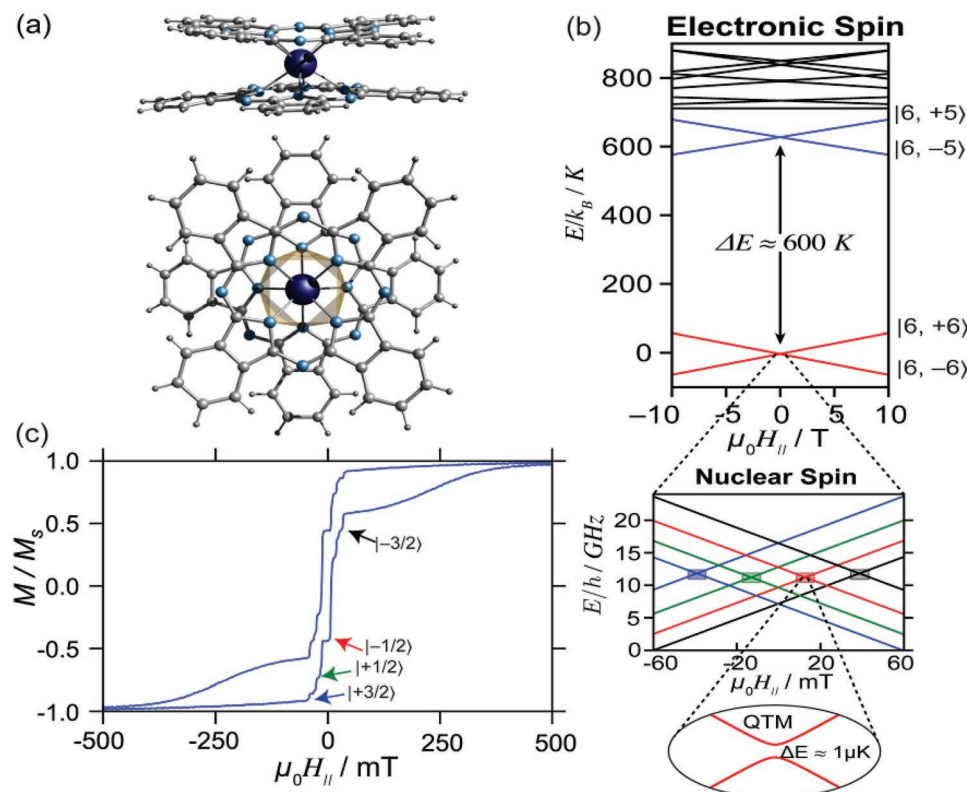


Figure 3. Single crystal X-ray diffraction study of $[^{159}\text{TbPc}_2]^{\pm 0}$ a) side and top view. b) Energy level diagram resulting from the strong spin orbit coupling of $^{159}\text{Tb(III)}$ and the ligand field exerted by the Pc groups. Zoomed regions show the effect of strong hyperfine interaction, which splits the $J_z = \pm 6$ state into four levels associated to $m_I = \pm \frac{1}{2}$ and $\pm \frac{3}{2}$ and avoided level crossing due to the mixing of states and tunnel splittings ΔE of $\approx 1 \mu\text{K}$. c) Hysteresis loop showing quantum tunneling (QTM) events associated to the nuclear spins. Panels a–c reproduced with permission.^[30] Copyright 2018, the Royal Society of Chemistry.

a dephasing time of $T^*_2 \approx 0.3 \text{ ms}$ for the nuclear spin qudit with four states and three transition frequencies.^[28,31] Hahn spin-echo experiments yielded a $T_2 \approx 1.2 \text{ ms}$. The experiment showed also that the resonance frequencies can be tuned electrically by means of the bias voltage,^[28] which is an important feature needed for more advanced quantum algorithms with several qudits. We reported proof-of-principle experiments with this system, in which the different implementations of quantum algorithms were tested.^[31,32]

Most recently, Grover quantum search algorithm was implemented into a single molecule transistor featuring a $^{159}\text{TbPc}_2$ qudit (Figure 4).^[31] Grover's quantum algorithm, proposed first by Lov Grover in 1996, a scientist at Bell Labs, is intended to find an element in an unsorted list or large data base with N entries in $O(N^{1/2})$ time and using $O(\log N)$ storage space (with O being any kind of observable and N the number of entries).^[33] Classical searching of an unsorted database requires a linear search algorithm, i.e., $O(N)$ in time. Grover's quantum algorithm, which takes $O(N^{1/2})$ time, is the fastest possible algorithm for searching an unsorted database. It provides "only" a quadratic speedup, unlike other quantum algorithms, which can provide exponential speedup over their classical counterparts; however, quadratic speedup is considerable when N is large. Grover's algorithm is nondeterministic, in the sense that it gives the correct answer with high probability. By repeating the algorithm and using a target value, this probability can

be increased. As early as in 1998, Grover's quantum search algorithm was implemented in a nuclear magnetic resonance (NMR)-experiment using the nuclear spin of carbon-labeled chloroform $^{13}\text{C}^1\text{HCl}_3$ as a two-qubit platform.^[34] Following this strategy, it was shown that the $^{159}\text{TbPc}_2$ molecule can act as two qubit-system or qudit with $d = 4$, making it possible to address and detect single nuclear spin states using the QTM of the SMM and to observe long energy-level lifetimes. Noticeably, this coherent manipulation was achieved by means of electric fields only and it was implemented by constructing a quantum register via a multilevel Hadamard gate. The Grover sequence then allowed selection of the respective state of interest.^[28,33] The method presented is universal and can be implemented in any multilevel quantum system with nonequally spaced energy levels, thus paving the way for novel quantum search algorithms. These results show how the coherent control over a single nuclear spin embedded in a molecular spin transistor can be gained and read-out nondestructively.

Another molecular system to potentially act as qudit system is shown in Figure 5, where the carbamate formation from CO_2 and a lanthanide source in the presence of a secondary amine was explored leading to a lanthanide-carbamate cage with the formula $[\text{Dy}_4(\text{O}_2\text{CN}^i\text{Pr}_2)_{12}]^0$.^[34] Magnetic studies showed slow relaxation leading to the observation of hysteresis loops; the tetranuclear cage being an SMM. Detailed interpretation of the data revealed: i) the presence of two different exchange

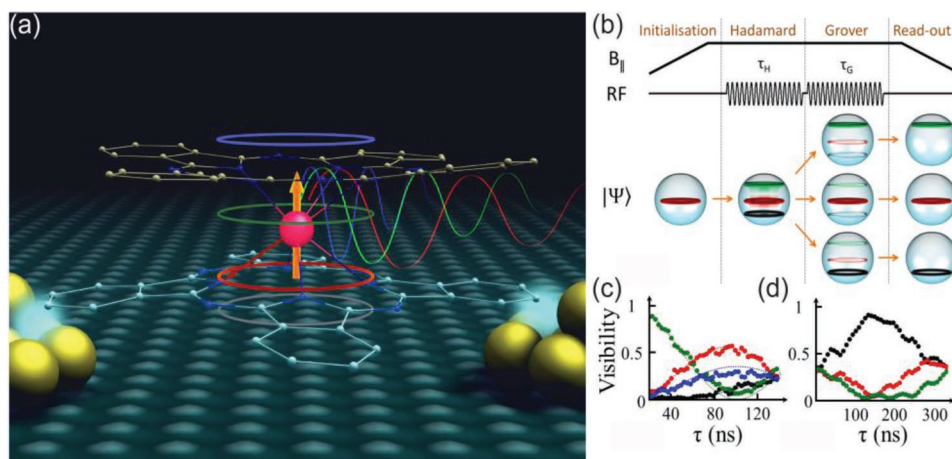


Figure 4. a) Schematic representation of $^{159}\text{TbPc}_2$ in a transistor configuration, where through conductance measurements, magnetic field sweeps, and radiofrequency pulses the individual nuclear spin states (depicted as colored rings: black $|l = -3/2\rangle$, red $|l = -1/2\rangle$, green $|l = +1/2\rangle$, blue $|l = +3/2\rangle$) are manipulated and read-out (via sweeping the electronic spin depicted as orange arrow with $J_z = \pm 6$); b) schematic representation of the Grover algorithm implemented by realization of i) initialization, ii) Hadamard gate, iii) Grover gate and final iv) read-out. c) Experimental data showing the evolution of the population in function of the Hadamard gate pulse length, while (d) represents the controlled decoherence of the Hadamard gate resulting in the respectively researched nuclear spin state (here black $|l = -3/2\rangle$). Panels b and c reproduced with permission.^[31] Copyright 2017, APS.

interactions, ferromagnetic and antiferromagnetic, and ii) the observation of exchange-bias quantum tunneling with two distinct sets of loops, attributable to ferromagnetic interactions between dysprosium (III) ions at longer distances and antiferromagnetic exchange between dysprosium ions at shorter distances. The coexistence of two applied-field direction dependent exchange pathways and the interesting magnetic

dynamics in $[\text{Dy}_4(\text{O}_2\text{CN}^i\text{Pr}_2)_{12}]^0$ could be of potential use in the above described quantum spintronic devices. The tuning and control of the quantum tunneling transitions upon manipulation of the field direction and/or the resonance fields would signify that the molecule could be exploited in four-qubit quantum computing algorithms, paving the way for higher-level qudits. In particular, when exploring the nuclear spins of the ^{163}Dy isotope,

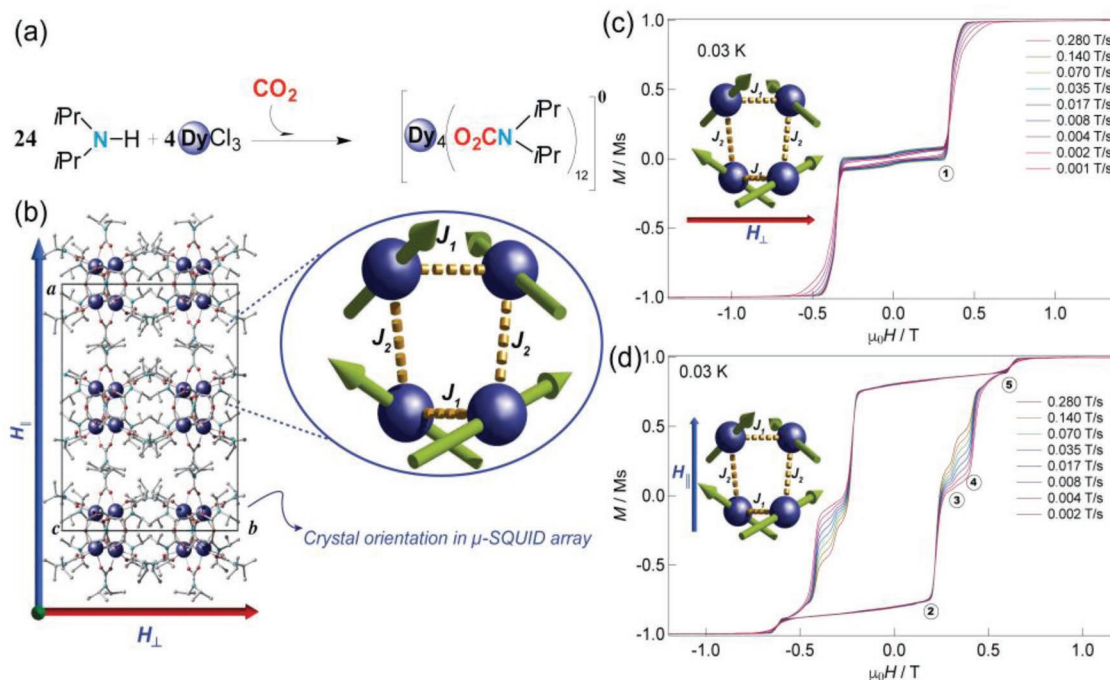


Figure 5. a) Reaction scheme for the synthesis of the carbamate SMM; b) Crystal packing and anisotropic magnetic axes of the dysprosium ions calculated employing an electrostatic potential; c,d) different μ -SQUID hysteresis loops obtained from a single crystal of $[\text{Dy}_4(\text{O}_2\text{CN}^i\text{Pr}_2)_{12}]^0$ with the field applied along and transverse to the anisotropic easy axis. Two different exchange pathways operate at molecular level, numbers 1–6 indicate the respective QTM events. Panels a–d reproduced with permission.^[34] Copyright 2017, the Royal Society of Chemistry.

four $I = 5/2$ qudits could be coupled to a Hilbert space with $d = (2I + 1)^4 = 1296$ (see Section 4.2).

4. Scaling of the Hilbert Space of Molecular Spin Qudits

Actually, $^{159}\text{TbPc}_2$ acts in the described experiments as multilevel qubit, also called spin “qudit,” based on the inherently entangled electronic and spin states of molecules. Actually, the qudit concept can be considered as a promising alternative to deliver exponential scalability of the available Hilbert space for quantum algorithms. Based on this property, qudits were proposed to play a key role in the realization of robust^[35a] and universal quantum computation.^[35b] The implementation of the Grover algorithm in a single molecular unit is possible because of the multilevel characteristics of the $^{159}\text{TbPc}_2$ molecular unit, in which the four nuclear spin states act as two quantum bits in one molecule. This observation clearly shows the advantage of the multilevel qudits ($d > 2$) over their two-level qubit ($d = 2$) counterparts, but the central challenge remains that the dimension d has to be increased to large numbers.^[36] In qudits entanglement and superposition can simultaneously be achieved in large dimensions, in so called Hadamard gates, requiring smaller numbers of quantum processing units.^[37,38] In addition, the multilevel character of the nuclear spin embodied in the lanthanide-based quantum magnets can be employed to directly perform quantum algorithms in a single unit. It becomes obvious that the available Hilbert space in qudits can increase faster than in qubits, following $d = (2I + 1)^n$ with I being the nuclear spin state and n the number of involved metal ions, vide supra.

However, to achieve state numbers needed to express eventually quantum supremacy, the quantum operation presented above has to be extended to alternative spin qubit devices dealing with an increased number of states. The great diversity of available molecular to act as qudits and with their inherent tunability could provide higher nuclear spin values that might afford much bigger databases for the field of molecular quantum computation.

An important requirement for the implementation of 2D electronic quantum bits in logic gates is the entanglement of these building blocks into arrays in order to produce higher order qubit geometries, ultimately allowing gate operations. In qudits, this can be achieved by magnetic coupling of the electronic spins. Several molecular materials have been proposed and studied as qudits building blocks and quantum gates because of their customizable chemical design. The molecules obtained would allow the processing of information at a quantum level due to the 2^N states generated by the magnetically coupled central atoms. Chemistry offers all necessary tools to achieve such a goal as illustrated by the chemically-engineered $\{\text{Cr}_7\text{Ni}\}$ unit, which could be used as CNOT and $\sqrt{\text{iSWAP}}$ gates,^[39] and a lanthanide dimer, which acts as a CNOT gate.^[40]

Unfortunately, operation with local qubits is not sufficient for creating quantum gates and global quantum evolutions, thus making correlated operations a necessity. The latter can be translated to a larger number of qudit aggregates, in chemical terms,

isotopological multinuclear complexes. Isotopological chemistry undoubtedly offers all the tools necessary to create such large qudit aggregates, which can ultimately be employed as universal quantum gates via ligand design. Isotopological chemistry also allows the metal centers to be exploited to create a larger number of states thus allowing for the production of large-scale qudits. The larger qudit state dimension will offer greater flexibility for different quantum applications.^[36] Moreover, the isotopological character of lanthanide complexes allows also to make “dummy” complexes containing no nuclear spin on the central atom to study of the effect of nuclear spin fluctuation in the transport of device applications. Another possibility is that, by excluding the nuclear spins embedded on the ligands, it will be possible to isotopologically engineer the ligand field around the central atom bearing the Hilbert space, thereby influencing their quantum tunneling and decoherence rates. Nuclear spins in the immediate environment of the lanthanide may be responsible for the shortening of the coherence time T_2 .^[28]

In conclusion, molecular systems clearly offer the advantage to chemically design their ground state. Thus, it was shown that the nuclear spins embedded in an SMM could act as nuclear spin qudits with the advantage of being extremely robust to environmental fluctuations. Driven by these arguments, we endeavor to create larger nuclear spin qudits by chemical design of the nuclear states embedded in the lanthanides. To achieve this, we propose in the following two main strategies: i) the enlargement of the nuclear states by employing isotopically enriched lanthanide sources and ii) the expansion of the nuclear spin states via coupling of the electronic states. The enlarged Hilbert space (i.e., number of nuclear states available for computation) will allow, in principle, for the realization of more complex algorithms in a single molecular unit.

4.1. Linear Scaling: Nuclear Spin Multiplicity in Mononuclear Isotopologues

As described above, the nuclear spins embedded in the lanthanide centers comprising the magnetic behavior of SMMs can be used to exploit the quantum effects associated to the nuclear states to implement quantum-computing algorithms. However, there are two strong requirements to allow a magnetic molecule to act as molecular spin qudit in quantum information schemes: 1) The presence of a strong magnetic anisotropy of SMMs is a precondition for the successful initialization, manipulation, and read-out of the nuclear-state based quantum information. 2) The hyperfine interaction between the electronic lanthanide spin J and the nuclear spin I has to exhibit a quadrupolar term P to allow the selective addressing of the different nuclear spin states levels by external microwave pulses. Concerning the first point, although ^{159}Tb -based SMMs seem promising candidates as nuclear spin qubits, the non-Kramers character of the Tb(III) ion has led to a very limited number of examples of Tb(III)-based SMMs with satisfyingly strong magnetic anisotropy. Instead, the much more favorable Kramers character of Dy(III) often produces a well isolated ground doublet state, making it the leading lanthanide for the synthesis of SMMs. However, before the advantageous magnetic properties of Dy(III) ions can be used, one challenge has to mas-

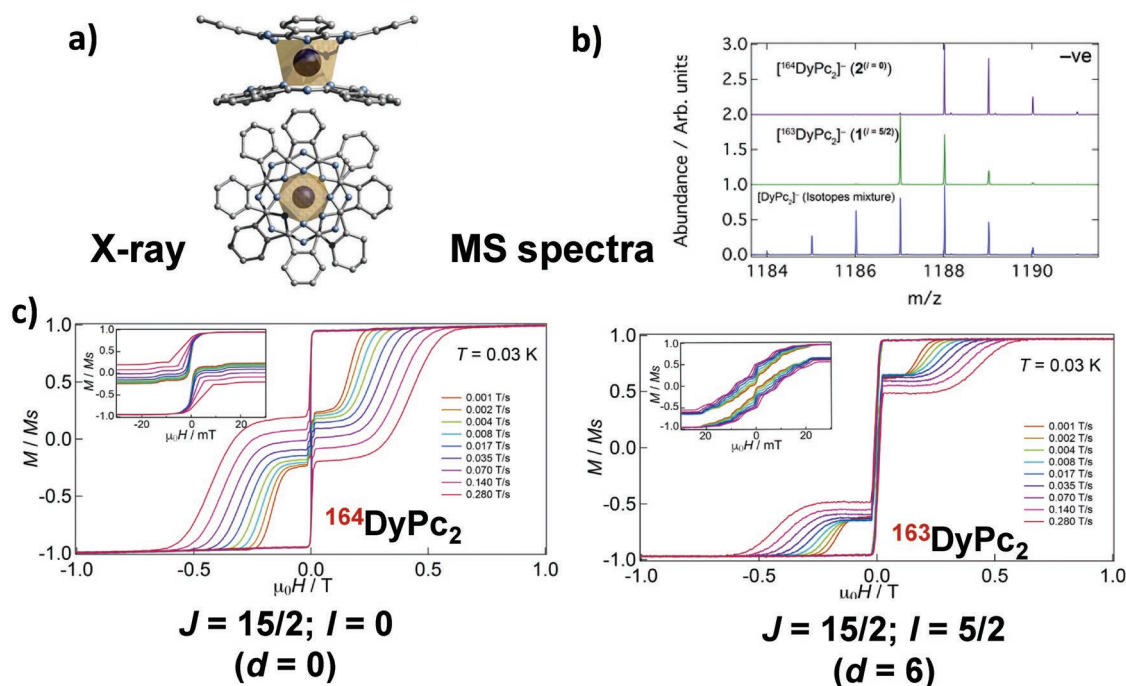


Figure 6. a) Realization of mononuclear $^{163/164}\text{DyPC}_2$ isotopologues showing an identical single-crystal x-ray structure but b) different high-resolution mass spectrometry (HR-MS) of the isotopologues $\text{Et}_4\text{N}[\text{DyPC}_2]^-$ ($I = 0$) and $\text{Et}_4\text{N}[\text{DyPC}_2]^-$ ($I = 5/2$) with the mass difference of $m/z = 1$ corresponding to one neutron c) μ -SQUID data for both complexes, showing for both $\text{Et}_4\text{N}[\text{DyPC}_2]^-$ ($I = 0$) and $\text{Et}_4\text{N}[\text{DyPC}_2]^-$ ($I = 5/2$) SMM character but revealing a significant difference in hysteresis and in the hyperfine-driven quantum tunneling event associated to the nuclear spins embedded in the 163-dysprosium (III) ion. Panels a–c reproduced with permission.^[43]

tered: whereas $^{159}\text{Tb(III)}$ contains a single nuclear spin isotope, $I = 3/2$, with 100% natural abundance, the natural composition of Dy(III) comprises seven isotopes, possessing two different nuclear spin states, $I = 0$ and $5/2$. Recently, in the quest for improved SMM properties, some research groups exploited the synthesis of isotopically enriched Dy-SMMs to improve the magnetic hysteresis width by excluding nuclear spins.^[41] The utilization of $^{164}\text{Dy(III)}$ ($I = 0$) led to the observation of enlarged hysteresis loops at zero field, in comparison to SMMs obtained from the naturally occurring isotopic mixture. On the contrary, investigation of the nuclear spin bearing materials, their quantum properties and their basic studies for their application as nuclear spin qubits remain scarce.^[42]

In the search for isotope-based quantum effects in SMMs we have prepared two isotopologue molecules: $\text{Et}_4\text{N}[\text{DyPC}_2]^-$ with $I = 0$ and $\text{Et}_4\text{N}[\text{DyPC}_2]^-$ with $I = 5/2$ (Et_4N^+ being the tetraethylamino cation). Both isotopologues are SMMs, however their relaxation times as well as their magnetic hystereses widths differ considerably (Figure 6a–c). QTM (via their energy level crossings) was found for both systems by ac-susceptibility and μ -SQUID measurement.^[43] Concerning the second strong requirement, the presence of the quadrupolar term of the hyperfine coupling to guarantee an unequal energy spacing of the nuclear spin states to be addressed, the μ -SQUID loops for $[\text{DyPC}_2]^-$ revealed a staircase-like structure between $\approx \pm 20$ mT (see Figure 6c right), which is clear evidence of hyperfine-induced QTM events. In this case, QTM arises from the nonzero transverse terms under C_4 symmetry, which allow the admixtures of the off-diagonal elements that mix the $|J_z\rangle$ and the $|J_z - 4\rangle$ levels affording an

avoided crossing at zero field.^[43] This crossing is further split, due to the entanglement between the $|13/2\rangle$ electronic and the $I = 5/2$ nuclear spin in $[\text{DyPC}_2]^-$. A total of 36 level crossings are expected (Figure 4c), whereby most of the tunneling events can be explained by a hyperfine interaction (A_{hf}) and a quadrupole term (P), employing a Hamiltonian of the form

$$H = H_{\text{lf}} + g_J \mu_0 \mu_B J \cdot H + A_{\text{hf}} I \cdot J + P(I_z^2 - 1/3(I+1)I) \quad (1)$$

where H_{lf} is the LF Hamiltonian ($H_{\text{lf}} = \alpha A_2^0 O_2^0 + \beta(A_4^0 O_4^0 + A_4^4 O_4^4) + \gamma(A_6^0 O_6^0 + A_6^4 O_6^4)$) being α , β , and γ the Stevens constants. The second term describes the Zeeman interaction, followed by the hyperfine and the quadrupole interaction parameters. Employing the reported LF values,^[44] a hyperfine parameter, $A_{\text{hf}} = 0.0051 \text{ cm}^{-1}$ and a quadrupole value of $P = 0.014 \text{ cm}^{-1}$, we are able to reproduce the observed events.^[43] Altogether, the presence of multiple nuclear-spin-driven QTM events as well as the determination of the hyperfine coupling and the nuclear quadrupole splitting prove that $[\text{DyPC}_2]^-$ could be potentially used as qudit with an increased Hilbert space of $d = 6$ in QIP schemes. This result provides a first example of how the spin ground state can be engineered by coordination chemistry of isotopes, or isotopological chemistry, employing nuclear spin isotopes.

In principle, just by replacing the central atom in the $^{\text{A}}\text{LnPC}_2$ spin qudit by suited isotopes, a linear increase of the dimension of the Hilbert space can be achieved (see Table 1). The isotopic nature of the central ion could be modified in order to yield a series of isotopologues of the following stable isotopes (among others): $^{\text{A}}\text{Ln} = ^{171}\text{Yb}$ ($I = 1/2$); ^{157}Gd ($I = 3/2$);

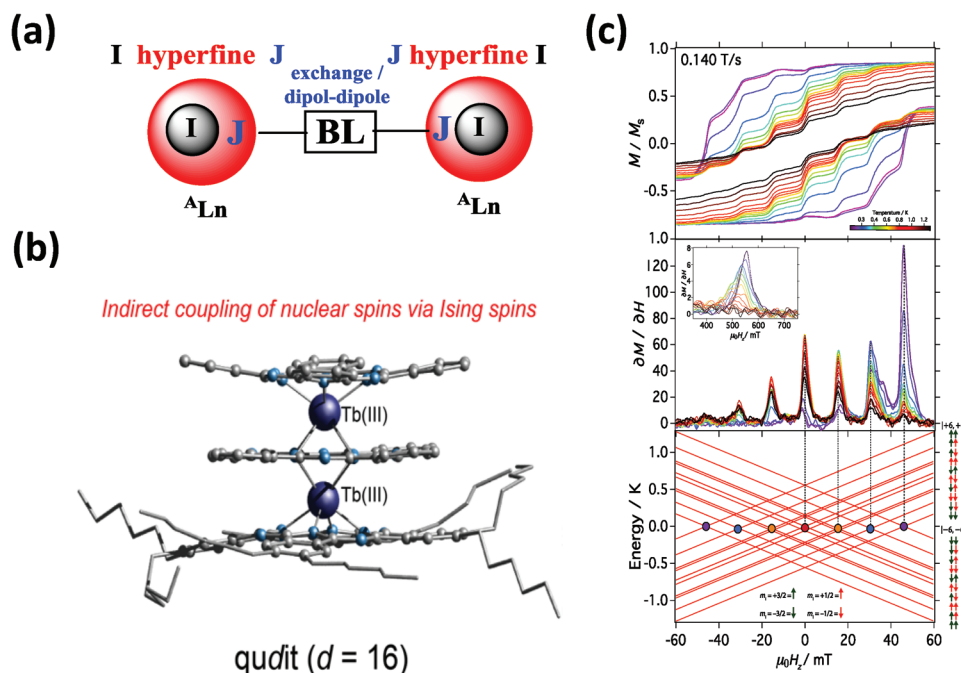


Figure 7. a) Schematic representation of the indirect coupling of the nuclear spin states I via the electronic states J and through a bridging ligand (BL) b) Structural data of the $\text{Pc}^{159}\text{TbPc}^{159}\text{TbPc}^*$ spin qudit together with c) its μ -SQUID data. The observed quantum tunneling of magnetization (QTM) events (above) and its derivate (middle) correspond to the Zeeman diagram of a spin qudit with $d = (2 \times 3/2 + 1)^2 = 16$ (below). Panels in c reproduced with permission.^[47] Copyright 2018, the American Chemical Society.

^{161}Dy ($I = 5/2$); ^{163}Dy ($I = 5/2$); and ^{167}Er ($I = 7/2$). It has to be emphasized again, to ensure addressability by radiofrequency pulses of different energy, the presence of quadrupole interaction parameter P in the chosen isotopes is of primordial importance (see Equation (1)). To project how far the nuclear spin approach could remain valid, the use of the highest nuclear spin multiplicity available in the periodic system with $I = 9/2$ for ^{93}Nb would give a $^{93}\text{NbPc}_2$ complex with a maximum achievable dimension of the Hilbert space of $d = 10$.^[45]

4.2. Exponential Scaling: Coupling of Nuclear Spin States

The second approach to increase the Hilbert space of a qudit, which means on molecular level the multiplicity of low-lying

Table 1. Examples of linear scaling of the dimension d of the Hilbert space of the mononuclear $^A\text{Ln}_n\text{Pc}_2$ qudit ($n = 1$) by choosing nuclear spin isotopes ^ALn as central atom bearing a nuclear spin I .

$^A\text{Ln}_n\text{Pc}_2$ qudit ($n = 1$)		
isotope ^ALn	Nuclear spin I	$d = (2I + 1)^n$
^{164}Dy	0	1
^{171}Yb	1/2	2
^{157}Gd	3/2	4
^{163}Dy	5/2	6
^{167}Er	7/2	8
$^{93}\text{Nb}^a)$	9/2	10

^{a)}Transition metal.

magnetic states, is based on the synthesis of multinuclear lanthanide SMMs, where dipolar or exchange interactions between the different lanthanide central ions would lead to an increased multiplicity of states (Figure 7a). Future applications of molecular units in quantum information technologies will require a fine control of the position of quantum states at the single molecule level. This includes the choice of each functional element, the intramolecular interaction, and the robustness of molecules when dispersed on a substrate. With this in mind, we studied first a hetero-metallic phthalocyaninato complex including two different lanthanides in each moiety, namely $\text{Pc}^{\text{Mix}}\text{DyPc}^{159}\text{TbPc}^*$ (Pc being phthalocyanines; and Pc^* being 2,3,9,10,16,17,23,24-octa-hexyl-substituted phthalocyanines, Dy in its naturally abundant isotopes' mixture).^[46] Full magnetic characterization was performed down to the mK temperature range on bulk microcrystals by means of AC susceptibility, DC magnetization (including μ -SQUID) and specific heat measurements revealing sizeable interaction between the two lanthanides. Data analysis shows the presence of two thermally activated regimes and quantum tunneling particularly active at very low temperatures. Due to the intramolecular interaction, mostly of dipolar origin, the low temperature magnetization dynamics is dominated by a cotunneling process. Isolated $\text{Pc}^{\text{Mix}}\text{DyPc}^{159}\text{TbPc}^*$ molecules dispersed on HOPG and the Au surface by liquid phase deposition are proven to maintain unchanged in their main chemical nature. Opening of a small but sizable hysteresis loop at 1.8 K is directly observed on both ^{159}Tb and $^{\text{Mix}}\text{Dy}$ sites proving the retention of magnetization at the single molecule level after surface confinement.

In order to characterize the interaction between the two lanthanides in more detail, we investigated the low temperature

physics of the respective isotopically pure dinuclear ^{159}Tb complex, namely $\text{Pc}^{159}\text{TbPc}^{159}\text{TbPc}^*$ (Figure 7b). Structurally, each $^{159}\text{Tb(III)}$ metal ion exhibits a distorted D_{4d} local symmetry: one $^{159}\text{Tb(III)}$ is coordinated between the two Pc ligands with a CShM¹⁵ value of 1.593, while the other $^{159}\text{Tb(III)}$ metal ion, being sandwiched between one Pc and one Pc^* , a CShM of 2.553.^[47] The distance within the molecule between the two ^{159}Tb isotopes is 3.5230(8) Å as determined by X-ray diffraction, while the shortest intermolecular Tb...Tb distance is with 10.8571(7) Å much larger, thus intermolecular interactions are expectedly small. Static and dynamic SQUID measurements on a magnetically diluted sample revealed a small ferromagnetic dipolar coupling between the electronic spins $J = 6$ of the two $^{159}\text{Tb(III)}$ isotopes and the expected SMMs behavior showing a single Debye process. Moreover, subkelvin μ -SQUID studies on single crystals with the magnetic field applied parallel to its C_4 axis elucidated small interaction between the nuclear spins $I = 3/2$ embodied in the $^{159}\text{Tb(III)}$ metal ions. Notably, the hysteresis loops in the vicinity of $\mu_0 H_z = 0$ show a staircase-like structure with seven transitions occurring at 0, ± 15.4 , ± 30.4 , and ± 45.7 mT (see Figure 7c) and an additional broad transition is also obtained at ± 550 mT. The seven quantum tunneling transitions are very different compared to the situation in the mononuclear $[\text{TbPc}_2]^\pm$ complex,^[44] and also to some recently reported fused Pc-bridged Tb-dimers,^[48] where only four avoided level crossings are present, corresponding to the four nuclear states of Tb(III) ion, at ± 12 mT and ± 37 mT. These transitions are caused by the transverse crystal field terms ($B_4^4 O_4^4$ and $B_6^4 O_6^4$), arising from the small distortion of D_{4d} point group to C_4 , which are consequently influenced by the presence of the nuclear spins of the lanthanide isotope. The two independent $^{159}\text{Tb(III)}$ act as two separated quantum units and the observed steps can be assigned to the cotunneling of the electronic spin $J = 6$ of each unit, while the corresponding nuclear spin states are conserved.

The central hyperfine-driven QTM (hf-QTM) steps of the magnetization have previously been observed in other lanthanide systems,^[44] however, what makes the $\text{Pc}^{159}\text{TbPc}^{159}\text{TbPc}^*$ system unique is the collective behavior triggered by the small coupling interaction between the $^{159}\text{Tb(III)}$ isotopes. This interaction connects the nuclear spins, causing not just hf-QTM occurrences, as observed in the $[\text{TbPc}_2]^-$ SMM, but more importantly it increases the multiplicity of states allowing the QTM at more resonance field positions than four (see Figure 7c, top). Our results, in addition diverge with those of the exchange-bias driven QTM, where the resonance fields are shifted due to exchange with adjacent nuclei.^[49,50]

To understand the μ -SQUID results we consider the distorted nature of the $^{159}\text{Tb(III)}$ isotope, which imposes a C_4 symmetry characterized by ligand field Hamiltonian of the form

$$H_{\text{lf}}^i = \alpha A_2^0 O_2^0 + \beta (B_4^0 O_4^0 + B_4^4 O_4^4) + \gamma (B_6^0 O_6^0 + B_6^4 O_6^4) \quad (2)$$

where $i = 1$ or 2 (referring to each $^{159}\text{Tb(III)}$ isotope) and α , β , and γ are the Stevens coefficients, O_i^k are the equivalent Stevens operators and B_i^k are the ligand field parameters. To account for the nuclear spin embedded in the $^{159}\text{Tb(III)}$ isotope

and the effect of the magnetic field on the multiplicity of the m_j states, then three other terms are included

$$H_{\text{Tb}}^i = H_{\text{lf}}^i + g_j \mu_0 \mu_B J_z \cdot H_z + A_{\text{hf}} I \cdot J + P \left(I_z^2 - \frac{1}{3} (I+1) I \right) \quad (3)$$

In (Equation (3)) the second term describes the Zeeman interaction and the third and fourth term includes the important hyperfine (A_{hf}) and the quadrupole interaction (P) parameters, respectively. The LF parameters were taken from a closely related molecule.^[44,47] Due to the relatively close proximity of the $^{159}\text{Tb(III)}$ isotopes, both ions are connected by a weak dipolar interaction of the form

$$H_{\text{dip}} = - \left[3 (\mu_i r_{ij}) (\mu_j r_{ij}) / r_{ij}^5 - \mu_i \mu_j / r_{ij}^3 \right] \quad (4)$$

thus Hamiltonian for $\text{Pc}^{159}\text{TbPc}^{159}\text{TbPc}^*$ reads

$$H = H_{\text{dip}} + H_{\text{Tb}}^1 + H_{\text{Tb}}^2 \quad (5)$$

The energy ladder of $\text{Pc}^{159}\text{TbPc}^{159}\text{TbPc}^*$ could be calculated by exact diagonalization of the $(2J+1)^2(2I+1)^2 \times (2J+1)^2(2I+1)^2$ Hamiltonian (Equation (5)). Employing A_{hf} and P as parameters and fixing H_{dip} to $+3.21 \text{ cm}^{-1}$, the seven QTM events could be reproduced as observed in the μ -SQUID data. The hyperfine parameters could be determined with $P = 0.010 \text{ cm}^{-1}$ and $A_{\text{hf}} = +0.0215 \text{ cm}^{-1}$; assuming P and A_{hf} for both sites to be equal. In view of the future implementation of the Grover quantum search mechanism, the P parameter was found equal to the one found for the mononuclear $[\text{TbPc}_2]^-$ SMM, whilst the important quadrupolar splitting A_{hf} was determined larger than that obtained in the mononuclear case obtained.^[44] The Zeeman diagram obtained employing Equation (5) contains 100 crossings (Figure 7c bottom), however, from these, solely 7 truly allow the reversal of the electronic spins, due to the off-diagonal terms in the Hamiltonian, which couple the $|J_z\rangle$ and $|J_z - 4\rangle$ states. The many transitions observed in μ -SQUID traces can be rationalized as follows: in the terbium dimer both $^{159}\text{Tb(III)}$ isotopes are coupled by a dipolar and/or exchange interaction, thus the eigen states are expressed as $|J_z^a\rangle |J_z^b\rangle$. At the measuring temperatures of 40 mK, only the $| -6\rangle | I_z^a\rangle | -6\rangle | I_z^b\rangle$ states are populated; therefore, reversal of the electronic spins occurs at the allowed level crossings when sweeping the field from a high negative field to a positive one. Upon sweeping the field, the initial electronic state is $| -6\rangle | I_z^a\rangle | -6\rangle | I_z^b\rangle$ up to zero field, where a crossing between $| -6\rangle | \pm 1/2\rangle | -6\rangle | \mp 1/2\rangle$ and the $| +6\rangle | \pm 1/2\rangle | +6\rangle | \mp 1/2\rangle$ states occurs. Note that at zero field, it is also possible for the electronic spin to tunnel between the $| -6\rangle | \pm 3/2\rangle | -6\rangle | \mp 3/2\rangle$ to $| +6\rangle | \pm 3/2\rangle | +6\rangle | \mp 3/2\rangle$ states (red circle in Figure 7c bottom). The next allowed tunneling event occurs at ± 15.4 mT, where the reversal is allowed via the state $| -6\rangle | \pm 1/2\rangle | -6\rangle | \pm 1/2\rangle$ to $| +6\rangle | \pm 1/2\rangle | +6\rangle | \pm 1/2\rangle$ (orange circles in Figure 7c bottom, whilst at ± 30.4 mT the reversal occurs through $| -6\rangle | \pm 1/2\rangle | -6\rangle | \pm 3/2\rangle$ to $| +6\rangle | \pm 1/2\rangle | +6\rangle | \pm 3/2\rangle$ (blue circles in Figure 7c bottom). Finally, at ± 45.7 mT the electronic spins flip through $| -6\rangle | \pm 3/2\rangle | -6\rangle | \pm 3/2\rangle$ to $| +6\rangle | \pm 3/2\rangle | +6\rangle | \pm 3/2\rangle$ (purple circles in Figure 7c bottom). The intensity of the transitions (when sweeping the field from negative to positive), increases from right to left due to higher population at the

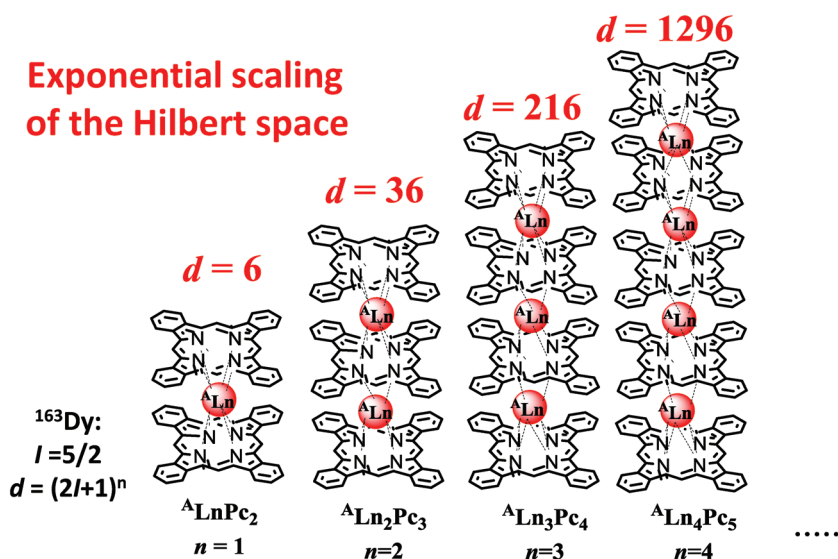


Figure 8. Conceptual scaling of the Hilbert space of the $A\text{Ln}_n\text{Pc}_{n+1}$ spin qudit ($I = 5/2$) with the example of $^{163}\text{Dy}_n\text{Pc}_{n+1}$ with $n = 1-4$ leading to exponential increase by $d = (2I + 1)^n$.

nuclear spin states at the lowest energy point. Therefore, we conclude that simultaneous spin reversals at specific avoided crossings are observed, as long as the nuclear spin states are conserved. The results show for the first time that the reversal of the electronic spins occurs via cotunneling at specific level crossings, induced by the exchange operating between the Tb(III) ions, thus opening the possibility of manipulation of the many nuclear spin states. This results in an exponential increase of the multiplicity of states, which would allow the creation of large directories, i.e., the realization of a molecular spin qudit with a potentially exploitable dimension of $d = 16$ (with $d = (2I + 1)^n$, where $n = 2$; $I = 3/2$).

Up to date, the single molecule magnets of the double-decker type with the highest nuclearity are reported up to Ln_4Pc_5 (Figure 8),^[51] however, without showing any evidence of QTM or nuclear spin interaction. This may be due the use of non-enriched Dysprosium metal sources; the mixture of seven different isotopes may hamper observation of QTM events. Also constitutes the central bridging ligand, a so called fused-Pc, namely bis{72,82,122,132,172,182-hexabutoxytribenzo[g,l,q]-5,10,15,20-tetraazaporphirino}[b,e] benzenato, an enlarged metal-to-metal distance. Beyond the Pc-ligand systems, lanthanide complexes incorporating the dianion of the 1,3,5,7-cyclooctatetreane ligand system, COT^{2-} represent an interesting alternative to access $\text{Ln}_n\text{Ln}_{n+1}$ complexes implying Eu, Ho, Yb, and Tb isotopes. In gas phase, Eu(II) complexes with nuclearities up to $n = 18$ were reported,^[52] while in solution $n = 4$ could be achieved.^[53] If the observed high nuclearities could be synthetically combined with the maximum nuclear spin reported in ^{93}Nb isotopes ($I = 9/2$),^[45] the Hilbert space of an hypothetical $^{93}\text{Nb}_{18}$ spin qudit would scale to $d = 10^{18}$; a number well above to all to date Hilbert spaces for any qubit material.

As shown in this chapter, strong requirements for the exponential scaling of the Hilbert space in nuclear spin based qudits are that i) the nuclear spins are coupled to at least one electronic spin, ii) the electronic spins are coupled between each other,

and iii) the tunnel splittings are not overlapping. For larger spin qudit systems, the energy level crossings might become rather close, a problem which is known under the term of “frequency crowding,” that is, it will become more and more difficult to select the right transition. This problem is inherent to all quantum systems and only future will tell us the most suitable one. However, in most of the quantum operations it will not be necessary to resolve all transitions. In most of the cases, the result of a quantum algorithm is projected in the end of the operation onto a certain number of states that only should be read out precisely.

5. Conclusion

Despite all breakthroughs, one prominent but not realized target in the novel quantum paradigm is the universal quantum computer exhibiting quantum supremacy, which would

allow the processing of information at quantum level for purposes not achievable with even the most powerful computer resources (e.g., search of unsorted databases, structural optimization of big-data analysis, secure quantum codes, etc.). One obvious challenge to be resolved toward the realization of such breakthrough technology concerns the scalability of the available Hilbert space. Recently, a proof-of-principle experiment was reported, in which the implementation of a quantum search algorithm (Grover’s algorithm) in a single-molecule nuclear spin qudit (with $d = 4$), known as TbPc_2 , was achieved. Here, the nuclear spins of the lanthanides are here used as a quantum register to execute quantum algorithms. To exploit such enlarged quantum registers improved read-out experiments have to be developed. In a first step, generalized Ramsey interferometry is used to explore the enlarged Hilbert space of a single nuclear spin qudits and to accumulate geometric phases. Two distinct transitions of a nuclear spin were addressed to measure the phase of an iSWAP quantum gate and to determine the coherence time of a 3-state superposition with 90 ms.^[32]

In this progress report, we have addressed the goal of scalability of the available Hilbert space (expressed by the qudit-dimension d) by synthesizing mono- and multinuclear lanthanide metal complexes as to act as quantum computing hardware. The synthesis of multinuclear large-Hilbert-space complexes is proposed to be carried out under strict control of the nuclear spin degree of freedom leading to isotopologues, whereby, in principle, indirect coupling between eighteen nuclear spin units of $I = 9/2$ (via their electron spins and via bridging ligands) will exponentially extend the Hilbert space available for quantum information processing ($d > 10^{18}$); a number well above to-date records for available Hilbert space of the Intel 49-qubit chip with a dimension of to $d = 2^{49}$ corresponding to potentially only ca. 10^{15} states.^[8]

Conflict of Interest

The authors declare no conflict of interest.

Keywords

Hilbert space, molecular spintronics, quantum algorithm, quantum computing

Received: October 15, 2018

Revised: January 9, 2019

Published online: February 25, 2019

- [1] A. Einstein, B. Podolsky, N. Rosen, *Phys. Rev.* **1935**, 47, 777.
- [2] E. Schrödinger, *Math. Proc. Cambridge Philos. Soc.* **1935**, 31, 555.
- [3] R. P. Feynman, *Int. J. Theor. Phys.* **1982**, 21, 467.
- [4] D. Deutsch, *Proc. R. Soc. A* **1985**, 400, 97.
- [5] P. W. Shor, *SIAM J. Comput.* **1997**, 26, 1484.
- [6] L. K. Grover, *Phys. Rev. Lett.* **1997**, 79, 325.
- [7] S. Lloyd, *Science* **1993**, 261, 1569.
- [8] <https://spectrum.ieee.org/tech-talk/computing/hardware/intels-49qubit-chip-aims-for-quantum-supremacy>, (accessed: August 2018).
- [9] <https://www.research.ibm.com/ibm-q>, (accessed: January 2019).
- [10] F. Jelezko, T. Gaebel, I. Popa, M. Domhan, A. Gruber, J. Wrachtrup, *Phys. Rev. Lett.* **2004**, 93, 130501.
- [11] L. Childress, M. V. G. Dutt, J. M. Taylor, A. S. Zibrov, F. Jelezko, J. Wrachtrup, P. R. Hemmer, M. D. Lukin, *Science* **2006**, 314, 281.
- [12] D. Loss, D. P. DiVincenzo, *Phys. Rev. A* **1998**, 57, 120.
- [13] K. C. Nowack, F. H. L. Koppens, Y. V. Nazarov, L. M. K. Vandersypen, *Science* **2007**, 318, 1430.
- [14] R. Prevedel, P. Walther, F. Tiefenbacher, P. Böhi, R. Kaltenbaek, T. Jennewein, A. Zeilinger, *Nature* **2007**, 445, 65.
- [15] G. J. Milburn, *Phys. Scr.* **2009**, T137, 014003.
- [16] J. J. Pla, K. Y. Tan, J. P. Dehollain, W. H. Lim, J. J. L. Morton, F. A. Zwanenburg, D. N. Jamieson, A. S. Dzurak, A. Morello, *Nature* **2013**, 496, 334.
- [17] J. J. Pla, K. Y. Tan, J. P. Dehollain, W. H. Lim, J. J. L. Morton, D. N. Jamieson, A. S. Dzurak, A. Morello, *Nature* **2012**, 489, 541.
- [18] A. Laucht, R. Kalra, S. Simmons, J. P. Dehollain, J. T. Muhonen, F. A. Mohiyaddin, S. Freer, F. E. Hudson, K. M. Itoh, D. N. Jamieson, J. C. McCallum, A. S. Dzurak, A. Morello, *Nat. Nanotechnol.* **2017**, 12, 61.
- [19] I. Chiorescu, Y. Nakamura, C. J. P. M. Harmans, J. E. Mooij, *Science* **2003**, 299, 1869.
- [20] a) J. Clarke, F. K. Wilhelm, *Nature* **2008**, 453, 1031; b) I. Bloch, *Nature* **2008**, 453, 1016;
- [21] R. Blatt, D. Wineland, *Nature* **2008**, 453, 1008.
- [22] L. Bogani, W. Wernsdorfer, *Nat. Mater.* **2008**, 7, 179.
- [23] a) T. F. Rønnow, Z. Wang, J. Job, S. Boixo, S. V. Isakov, D. Wecker, J. M. Martinis, D. A. Lidar, M. Troyer, *Science* **2014**, 345, 420; b) V. S. Denchev, S. Boixo, S. V. Isakov, N. Ding, R. Babbush, V. Smelyanskiy, J. Martinis, H. Neven, *Phys. Rev. X* **2016**, 6, 031015.
- [24] P. Macha, G. Oelsner, J.-M. Reiner, M. Marthaler, S. Andre, G. Schön, U. Hübner, H.-G. Meyer, E. Il'ichev, A. Ustinov, *Nat. Commun.* **2014**, 5, 5146.
- [25] E. Moreno-Pineda, T. Komoda, K. Katoh, M. Yamashita, M. Ruben, *Dalton Trans.* **2016**, 45, 18417.
- [26] M. Urdampilleta, S. Klyatskaya, J.-P. Cleuziou, M. Ruben, W. Wernsdorfer, *Nat. Mater.* **2011**, 10, 502.
- [27] R. Vincent, S. Klyatskaya, M. Ruben, W. Wernsdorfer, F. Balestro, *Nature* **2012**, 488, 357.
- [28] S. Thiele, F. Balestro, R. Ballou, S. Klyatskaya, M. Ruben, W. Wernsdorfer, *Science* **2014**, 344, 1135.
- [29] M. Ganzhorn, S. Klyatskaya, M. Ruben, W. Wernsdorfer, *Nat. Nanotechnol.* **2013**, 8, 165.
- [30] E. Moreno-Pineda, C. Godfrin, F. Balestro, W. Wernsdorfer, M. Ruben, *Chem. Soc. Rev.* **2018**, 47, 501.
- [31] C. Godfrin, A. Ferhat, R. Ballou, S. Klyatskaya, M. Ruben, W. Wernsdorfer, F. Balestro, *Phys. Rev. Lett.* **2017**, 119, 187702;
- [32] C. Godfrin, R. Ballou, S. Klyatskaya, M. Ruben, W. Wernsdorfer, F. Balestro, *Nat. Quant. Inform.* **2018**, 4, 53.
- [33] a) L. K. Grover, *Am. J. Phys.* **2001**, 69, 769; b) I. L. Chuang, N. Gershenfeld, M. Kubinec, *Phys. Rev. Lett.* **1998**, 80, 3408.
- [34] E. Moreno Pineda, Y. Lan, O. Fuhr, W. Wernsdorfer, M. Ruben, *Chem. Sci.* **2017**, 8, 1178.
- [35] a) D. P. O'Leary, G. K. Brennen, S. S. Bullock, *Phys. Rev. A* **2006**, 74, 032334; b) G. A. Paz-Silva, G. K. Brennen, J. Twamley, *Phys. Rev. A* **2009**, 80, 052318.
- [36] A. Morello, *Nat. Nanotechnol.* **2018**, 13, 5.
- [37] M. Mohammadi, A. Niknafs, M. Eshghi, *Quantum Inf. Process.* **2010**, 10, 241.
- [38] S. T. Merkel, G. Brennen, P. S. Jessen, I. H. Deutsch, *Phys. Rev. A* **2009**, 80, 023424.
- [39] G. A. Timco, S. Carretta, F. Troiani, F. Tuna, R. J. Pritchard, C. A. Muryn, E. J. L. McInnes, A. Ghirri, A. Candini, P. Santini, G. Amoretti, M. Affronte, R. E. P. Winpenny, *Nat. Nanotechnol.* **2009**, 4, 173.
- [40] G. Aromí, D. Aguilà, P. Gamez, F. Luis, O. Roubeau, *Chem. Soc. Rev.* **2012**, 41, 537.
- [41] a) Y. Kishi, F. Pointillart, B. Lefevre, F. Riobé, B. Le Guennic, S. Golhen, O. Cador, O. Maury, H. Fujiwara, L. Ouahab, *Chem. Commun.* **2017**, 53, 3575; b) F. Pointillart, K. Bernot, S. Golhen, B. Le Guennic, T. Guizouarn, L. Ouahab, O. Cador, *Angew. Chem., Int. Ed.* **2014**, 54, 1504.
- [42] J. M. Zadrozny, J. Niklas, O. G. Poluektov, D. E. Freedman, *J. Am. Chem. Soc.* **2014**, 136, 15841.
- [43] E. Moreno-Pineda, M. Damjanović, O. Fuhr, W. Wernsdorfer, M. Ruben, *Angew. Chem., Int. Ed.* **2017**, 56, 9915.
- [44] N. Ishikawa, M. Sugita, W. Wernsdorfer, *Angew. Chem., Int. Ed.* **2005**, 44, 2931.
- [45] a) M. P. Donzello, C. Ercolani, P. J. Lukes, *Inorg. Chim. Acta* **1997**, 256, 171; b) M. P. Donzello, C. Ercolani, A. Chiesi-Villa, C. Rizzoli, *Inorg. Chem.* **1998**, 37, 1347.
- [46] Y. Lan, S. Klyatskaya, M. Ruben, O. Fuhr, W. Wernsdorfer, A. Candini, V. Corradini, A. Lodi-Rizzini, U. del Pennino, F. Troiani, L. Joly, D. Klar, H. Wende, M. Affronte, *J. Mater. Chem. C* **2015**, 3, 9794.
- [47] E. Moreno-Pineda, S. Klyatskaya, P. Du, M. Damjanović, G. Taran, W. Wernsdorfer, M. Ruben, *Inorg. Chem.* **2018**, 57, 9873.
- [48] T. Morita, M. Damjanovic, K. Katoh, Y. Kitagawa, N. Yasuda, Y. Lan, W. Wernsdorfer, B. K. Breedlove, M. Enders, M. Yamashita, *J. Am. Chem. Soc.* **2018**, 140, 2995.
- [49] a) D. Aguila, L. A. Barrios, V. Velasco, O. Roubeau, A. Repolles, P. J. Alonso, J. Sese, S. J. Teat, F. Luis, G. Aromi, *J. Am. Chem. Soc.* **2014**, 136, 14215; b) M. D. Jenkins, Y. Duan, B. Diosdado, J. J. García-Ripoll, A. Gaita-Ariño, C. Giménez-Saiz, P. J. Alonso, E. Coronado, F. Luis, *Phys. Rev. B* **2017**, 95, 064423; c) M. Atzori, A. Chiesa, E. Morra, M. Chiesa, L. Sorace, S. Carretta, R. Sessoli, *Chem. Sci.* **2018**, 9, 6183.
- [50] L. Thomas, F. Lioni, R. Ballou, D. Gatteschi, R. Sessoli, B. Barbara, *Nature* **1996**, 383, 145.
- [51] K. Katoh, T. Morita, N. Yasuda, W. Wernsdorfer, Y. Kitagawa, B. K. Breedlove, M. Yamashita, *J. Chem-Eur. J.* **2018**, 24, 15522.
- [52] N. Hosoya, R. Takegami, J. Suzumura, K. Yada, K. Koyasu, K. Miyajima, M. Mitsui, M. Knickelbein, A. Yabushita, A. Nakajima, *J. Phys. Chem. A* **2005**, 109, 9.
- [53] T. Tsuji, N. Hososya, S. Fukuzawa, R. Sugiyama, T. Iwasa, H. Tsunoyama, H. Hamaki, N. Tokitoh, A. Nakajima, *J. Phys. Chem. C* **2014**, 118, 5896.